Evidence for stroke-induced neurogenesis in the human brain

Kunlin Jin[*†], Xiaomei Wang[†‡], Lin Xie[*], Xiao Ou Mao[*], Wei Zhu[‡], Yin Wang[§], Jianfeng Shen[¶], Ying Mao[‡], Surita Banwait[*], and David A. Greenberg[*‖]

*Buck Institute for Age Research, Novato, CA 94945; Departments of ‡Neurosurgery and §Neuropathology, Huashan Hospital, Fudan University, Shanghai 200040, China; and ¶Department of Neurosurgery, First Affiliated Hospital, Zhejiang Medical University, Zhejiang 310031, China

Experimental stroke in rodents stimulates neurogenesis and migration of newborn neurons from their sites of origin into ischemic brain regions. We report that in patients with stroke, cells that express markers associated with newborn neurons are present in the ischemic penumbra surrounding cerebral cortical infarcts, where these cells are preferentially localized in the vicinity of blood vessels. These findings suggest that stroke-induced compensatory neurogenesis may occur in the human brain, where it could contribute to postischemic recovery and represent a target for stroke therapy.

ischemia | stem cells | penumbra | infarct | vascular niche

Stroke, which usually results from occlusion of a cerebral artery leading to brain infarction, is among the commonest causes of death and disability in adulthood. However, many patients improve in the weeks to months following stroke, implying an innate capacity for brain repair. One means by which repair might be achieved is neurogenesis, which occurs in the adult human brain *in situ* (1), is increased in animal models of brain injury including stroke (2–5), and is associated with migration of newborn neurons to injured brain regions (6–9). Whether the human brain responds to stroke in a similar manner has not been determined, but it is important to examine this possibility because of the prospect that therapeutic enhancement of injury-induced neurogenesis might improve clinical outcome.

Results

Sections were obtained from human brain biopsies performed for the diagnosis of cerebral lesions that proved to be ischemic strokes (Table 1). The sections were stained with antibodies against markers of cell proliferation (proliferation-related Ki-67 antigen, Ki-67; *Saccharomyces cereviseae* minichromosome maintenance 2 homolog, MCM2; and proliferating cell nuclear antigen, PCNA) and neuronal lineage (doublecortin, DCX; TOAD/Ulip/CRMP family protein 4, TUC-4; embryonic nerve cell adhesion molecule, ENCAM; and βIII tubulin). Control specimens ($n = 6$), from the cerebral cortex of autopsied patients who died without brain pathology, contained ≤1 Ki-67-positive and no Ki-67/DCX-positive cells per mm². In stroke patients ($n = 6$), however, the cortical region adjacent to the infarct core (ischemic penumbra) contained 63 ± 16 Ki-67-positive cells and 10 ± 2 Ki-67/DCX-positive cells per mm² (mean ± SEM) (Table 1 and Fig. 1a). To confirm that Ki-67 labeling reflected recent cell proliferation, some sections were also stained for MCM2 (Fig. 1b) or PCNA (Fig. 1c), which were co-expressed in Ki-67-positive cells. Although dying neurons may aberrantly express cell-cycle proteins, fewer than 3% of Ki-67-positive cells in the ischemic penumbra showed evidence of caspase-3 cleavage, and these had distinctly abnormal nuclear morphology (Fig. 1d).

Because cell-cycle markers do not discriminate cells of different lineages, some sections were stained with lineage-specific markers. Markers expressed in new neurons, including DCX (Fig. 2a) and βIII tubulin (Fig. 2b), were localized to the ischemic penumbra. Moreover, DCX (Fig. 2c), βIII tubulin (Fig. 2d), and TUC-4 (Fig. 2e) were detected in cells that also expressed Ki-67, and multiple immature neuronal markers were expressed in a given cell (Fig. 2f), confirming that these were newborn neurons. Consistent with this interpretation, some Ki-67/DCX-positive cells exhibited a migratory phenotype consisting of an elongated cellular profile with a leading edge and trailing nucleus (Fig. 2g).

In the hippocampal dentate gyrus (which, together with the subventricular zone, accounts for most neurogenesis in the adult brain), new neurons arise in proximity to blood vessels, which are thought to provide a "vascular niche" that supports their proliferation (10). A similar relationship was observed in stroke brain specimens, in which DCX-positive cells tended to cluster near blood vessels labeled with antibodies against nestin (Fig. 3a), von Willebrand factor (Fig. 3b), or vascular smooth muscle actin (Fig. 3c). This finding may relate to observations that vascular endothelial cells promote neurogenesis *in vitro* (11) and that vascular endothelial growth factor, which stimulates the proliferation of neurons as well as endothelial cells (12), is induced in the brain after stroke (13). However, whether these new neurons arise locally or migrate from canonical neuroproliferative regions such as the subventricular zone cannot be resolved on the basis of biopsies restricted to the ischemic brain area.

Discussion

Neurogenesis persists in the adult mammalian brain, where it can be stimulated by physiological factors, such as growth factors and environmental enrichment, and by pathological processes, including ischemia and neurodegeneration. Although these influences are more difficult to demonstrate in humans than in experimental animals, evidence for injury-induced human neurogenesis has been presented previously in Huntington's disease (14) and Alzheimer's disease (15). Here, we report similar evidence for stroke-induced neurogenesis in human brain. Standard methods used to detect neurogenesis in animals, such as the administration of BrdU or GFP-expressing viral vectors, cannot be used in humans. Therefore, we relied on the expression of endogenous-cell-proliferation markers and neuronal-lineage markers to identify putative newborn neurons in the cortical ischemic penumbra of patients with stroke. These markers have limitations in that their relationship to neurogenesis has been characterized in most detail in rodents, and some of them may also be expressed in

---

Table 1. Clinical and immunohistological features in patients with stroke

Patient no.	Age, yr	Sex	Main symptoms	Duration, d	Stroke location	Ki-67(+), cells per mm^2 (mean ± SEM)	Ki-67/DCX(+), cells per mm^2 (mean ± SEM)
1	65	M	R hemianopia R hemiparesis R hemisensory loss	40	L parietal	36 ± 7	6 ± 6
2	45	M	Headache Aphasia	14	L temporo-occipital	62 ± 24	11 ± 7
3	54	F	Headache L hemiparesis	38	R parietal	109 ± 21	11 ± 3
4	66	M	L hemiparesis L hemisensory loss	42	R parietal	48 ± 10	11 ± 3
5	34	M	Headache	5	R occipital	11 ± 3	3 ± 3
6	74	F	R hemiparesis	32	L parietal	112 ± 12	17 ± 8

Cells were counted in three ×400 fields from the cortical ischemic penumbra, per patient. Duration is the time from onset of symptoms to biopsy. M, male; F, female; R, right; L, left.

injured cells. However, we observed cells that stained for multiple early neuronal markers, showed normal nuclear morphology, did not stain for caspase-cleavage products, had features consistent with a migratory cell phenotype, were present in the ischemic penumbra but not in the ischemic core (where injured cells would be expected to be found), and were situated preferentially in the vicinity of patent (erythrocyte-containing) blood vessels (which is not where ischemic cells
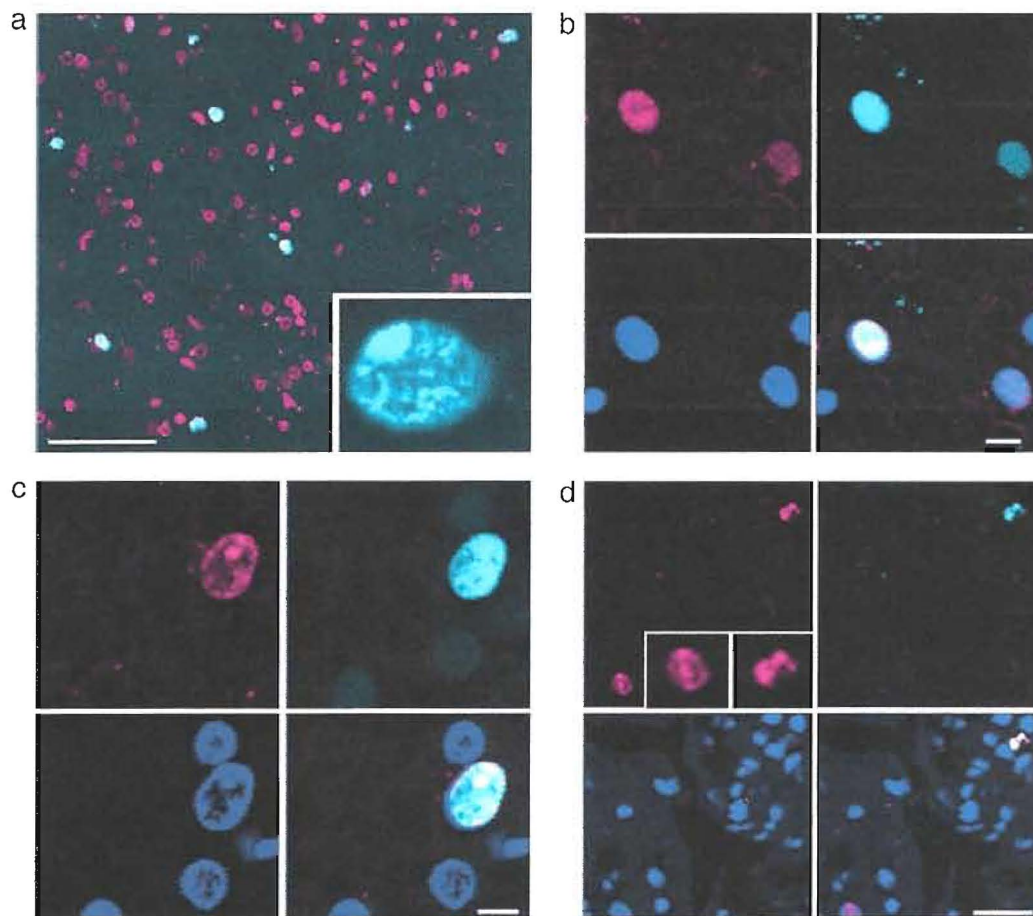

Fig. 1. Proliferative status of cells in the ischemic penumbra of human cerebral cortex after stroke. (*a*) Nuclei stained for the cell proliferation marker Ki-67 (green) are present in the ischemic penumbra, where TOTO-3 (red) has been used to counterstain all nuclei. (Scale bar, 150 μm.) (*Inset*) Ki-67-stained nucleus shown at higher magnification. (*b*) Ki-67 (red) (*Upper Left*) is colocalized with the cell proliferation marker MCM2 (green) (*Upper Right*) in the nucleus of a cell in the ischemic penumbra. (Scale bar, 10 μm.) (*c*) Ki-67 (red) (*Upper Left*) is colocalized with the cell proliferation marker PCNA (green) (*Upper Right*) in the nucleus of a cell in the ischemic penumbra. (Scale bar, 5 μm.) (*d*) Ki-67 (red) (*Upper Left*) colocalizes with a cell-death marker, the 17- to 20-kDa cleavage product of caspase-3 (green) (*Upper Right*) in cells with misshapen nuclei (top right corner of each panel and *Right Inset*), but not in cells with normal-appearing nuclei (bottom left corner of each panel and *Left Inset*). (Scale bar, 10 μm.) (*b–d*) *Bottom Left* and *Right* panels show DAPI-stained nuclei and merged images, respectively.

NEUROSCIENCE

Fig. 2. Neuronal character of cells in the ischemic penumbra of human cerebral cortex after stroke. (a) The early neuronal marker DCX (green) is expressed in the cytoplasm of numerous cells in the ischemic penumbra, where its expression does not overlap with that of the astroglial marker GFAP (red). (Scale bar, 150 μm.) (b) The neuronal marker βIII-tubulin (red) is highly expressed in the ischemic penumbra (center of panel), is less highly expressed in adjacent normal cortex (top of panel), and is absent in the ischemic core (bottom of panel). (Scale bar, 200 μm.) (c) DCX (green) is expressed in the cytoplasm of a cell with Ki-67-positive (red) nucleus. (Scale bar, 5 μm.) (d) βIII-tubulin (red) is expressed in the cytoplasm of a cell with Ki-67-positive (green) nucleus. (Scale bar, 7 μm.) (e) TUC-4 (red) is expressed in the cytoplasm of a cell with Ki-67-positive (green) nucleus. (Scale bar, 5 μm.) (f) ENCAM (red), DCX (green), and TUC-4 (purple) are colocalized; the nucleus is counterstained with DAPI (blue). (Scale bar, 10 μm.) (g) A cell with a Ki-67-stained nucleus (red) and DCX-positive cytoplasm (green) exhibits characteristic migratory morphology, with a leading process and trailing nucleus; nuclei are counterstained with DAPI (blue).
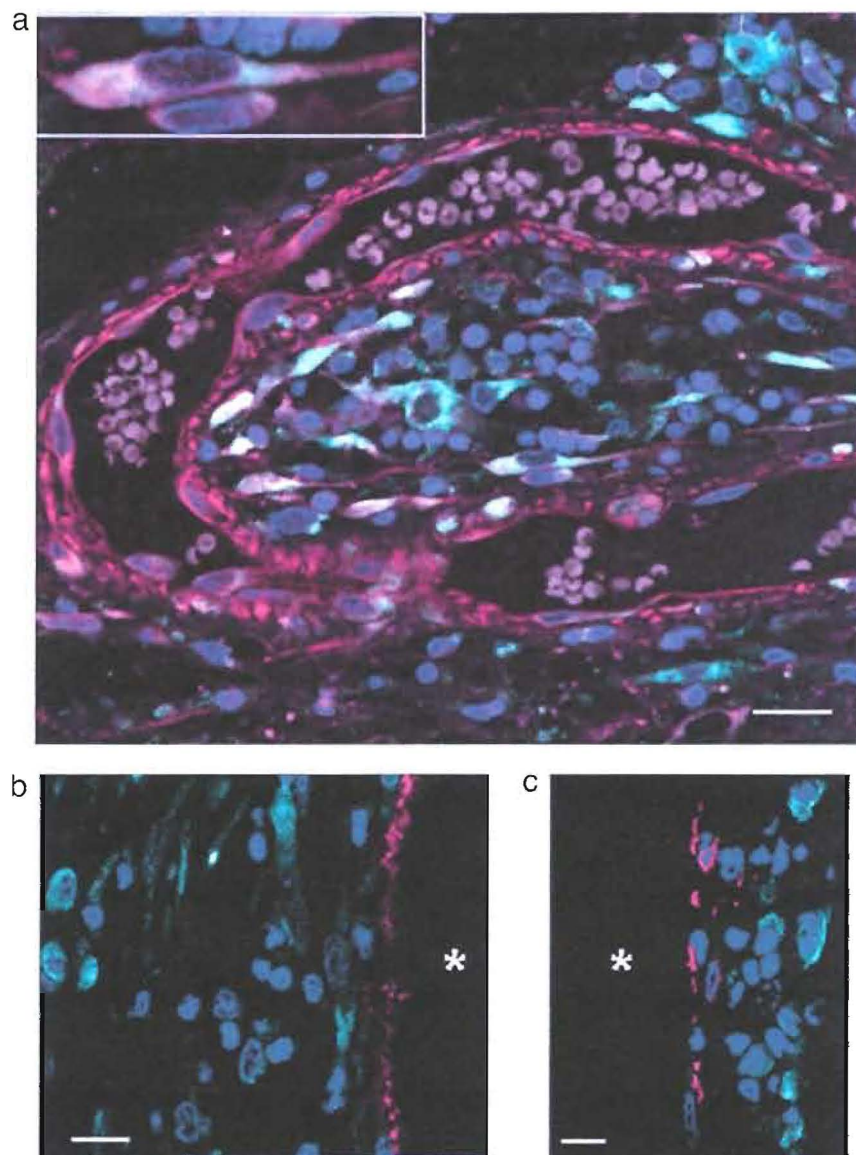
Fig. 3. Vascular niche for stroke-induced neurogenesis in human cerebral cortex. (*a*) A section stained for DCX (green), TUC-4 (purple), and nestin (red) and counterstained with DAPI (blue) shows DCX- and TUC-4-positive cells, some with the elongated morphology observed in migrating neurons (*Inset*), in clusters in the vicinity of a capillary that contains erythrocytes. (Scale bar, 20 μm.) (*b*) DCX-positive cells (green) are in the vicinity of, but distinct from, von Willebrand factor-positive endothelial cells (red); nuclei are counterstained with DAPI (blue). *, vessel lumen. (Scale bar, 15 μm.) (*c*) DCX-positive cells (green) are in the vicinity of, but distinct from, α_2-actin-positive vascular smooth muscle cells (red); nuclei are counterstained with DAPI (blue). *, vessel lumen. (Scale bar, 15 μm.)

would be anticipated). It is possible that all of these attributes are associated with ischemic injury rather than neurogenesis, but it seems unlikely.

In rodent models of stroke, the source of new neurons that migrate to ischemic brain areas appears to be the subventricular zone (6–9). In human biopsy specimens, the source of these cells is unclear, but their perivascular location may provide clues. One possibility is that newborn neurons migrate from elsewhere (such as the subventricular zone), using blood vessels as scaffolds for migration or as destination markers. Alternatively, these neurons could arise locally, although whether neurogenesis can occur *in situ* in primate cerebral neocortex is controversial (16, 17). The extent to which stroke-induced neurogenesis in human brain results in the production of functional neurons with the capacity to integrate into brain circuitry is also uncertain and is not addressed by our findings.

Several drugs can stimulate neurogenesis in the dentate gyrus or subventricular zone of ischemic rodent brain, including statins (18) and medications used to treat erectile dysfunction (19). Because none of the patients we studied was known to have taken any of these drugs, the increased neurogenesis we observed is unlikely to have been drug-induced. On the other hand, the ability of drugs and environmental alterations to promote neurogenesis suggests clinical interventions that might be used to enhance this process. Although its functional impact is as yet unknown, postischemic neurogenesis in the human brain may represent both an endogenous repair mechanism and a therapeutic target for stroke.

Materials and Methods

Human Brain Tissue. Brain specimens from patients aged 25–48 years and without clinical or postmortem evidence of neurolog-

ical disease ($n = 6$) were obtained at autopsy, and human stroke specimens ($n = 9$) were obtained at biopsy performed for diagnostic purposes, with informed consent and in accordance with protocols approved by the Institutional Research Review Board at Huashan Hospital of Fudan University, China. Cerebral cortical infarcts were confirmed by histopathology in six of nine patients, who were included in the present study; the remaining three of nine biposied patients were excluded because of other diagnoses (one each with cerebellar infarct, intracerebral hemorrhage, and intraventricular hemorrhage).

Immunohistochemistry. Tissues were postfixed in paraformaldehyde for 24 h, incubated with 30% sucrose for 3 days, and embedded in paraffin; 6-μm sections were cut on a microtome and stored at room temperature. Sections were deparaffinized with xylene and rehydrated with ethanol. Peroxidase activity was blocked with 1% H_2O_2, and sections were treated with citrate buffer (pH 6.0) (Zymed, Carlsbad, CA) at 96°C for 30 min, cooled for 25 min, and incubated in blocking buffer (2% horse serum/0.2% Triton X-100/0.1% BSA in PBS) for 1 h at room temperature. Primary antibodies used were mouse monoclonal anti-Ki-67 antigen (1:50; Novocastra, Newcastle upon Tyne, U.K.), rabbit anti-Ki-67 antigen (1:100; Zymed), goat anti-MCM2 (1:100; Santa Cruz Biotechnology, Santa Cruz, CA), mouse monoclonal anti-PCNA (1:200; Chemicon, Temecula, CA), rabbit anti-cleaved caspase 3 (1:200; BD PharMingen, San Diego, CA), affinity-purified goat anti-DCX (1:200; Santa Cruz Biotechnology), rabbit anti-GFAP (1:1,000; Sigma, St. Louis, MO), mouse monoclonal anti-βIII-tubulin (TUJ1, 1:250; Covance, Berkeley, CA), rabbit polyclonal anti-TUC-4 (1:10,000; Chemicon), mouse monoclonal anti-ENCAM (1:500; Chemicon), mouse monoclonal anti-human-specific nestin (1:200; Chemicon), rabbit anti-von Willebrand factor (1:500; Chemicon), and mouse monoclonal anti-α_2- (vascular smooth muscle) actin (1:100; Maine Biotechnology, Portland, ME).

Primary antibodies were added in blocking buffer and incubated with sections at 4°C overnight. The secondary antibodies were Alexa Fluor 488-, 594-, or 647-conjugated donkey anti-mouse, anti-goat, or anti-rabbit IgG (1:200–500; Molecular Probes, Carlsbad, CA). Nuclei were counterstained with DAPI using proLong Gold antifade reagent or with TOTO-3 (all from Molecular Probes), and fluorescence signals were detected with Nikon (Melville, NY) PCM-2000 laser-scanning confocal microscopy at excitation/emission wavelengths of 650/668 nm (Alexa Fluor 647, far red), 590/617 nm (Alexa Fluor 594, red), 495/519 nm (Alexa Fluor 488, green), or 360/400 nm (DAPI, blue). Slides were examined with an LSM 510 NLO confocal scanning system mounted on an Axiovert 200 inverted microscope (Carl Zeiss, Oberkochen, Germany) equipped with a two-photon Chameleon laser (Coherent, Santa Clara, CA). Images were acquired using LSM 510 imaging software (Carl Zeiss). Four-color images were scanned using argon, 543 HeNe, 633 HeNe, and Chameleon (750–780 nm for DAPI) lasers. IMARIS (Bitplane, Zurich, Switzerland) imaging software was used for three-dimensional image reconstruction. Controls included omitting or preabsorbing primary antibodies or omitting secondary antibodies. Cells were counted blindly in three 425×280-μm fields per sample under ×400 magnification.

1. Eriksson, P. S., Perfilieva, E., Bjork-Eriksson, T., Alborn, A. M., Nordborg, C., Peterson, D. A. & Gage, F. H. (1998) *Nat. Med.* **4**, 1313–1317.
2. Liu, J., Solway, K., Messing, R. O. & Sharp, F. R. (1998) *J. Neurosci.* **18**, 7768–7778.
3. Gu, W., Brannstrom, T. & Wester, P. (2000) *J. Cereb. Blood Flow Metab.* **20**, 1166–1173.
4. Jin, K., Minami, M., Lan, J. Q., Mao, X. O., Batteur, S., Simon, R. P. & Greenberg, D. A. (2001) *Proc. Natl. Acad. Sci. USA* **98**, 4710–4715.
5. Zhang, R. L., Zhang, Z. G., Zhang, L. & Chopp, M. (2001) *Neuroscience* **105**, 33–41.
6. Arvidsson, A., Collin, T., Kirik, D., Kokaia, Z. & Lindvall, O. (2002) *Nat. Med.* **8**, 963–970.
7. Parent, J. M., Vexler, Z. S., Gong, C., Derugin, N. & Ferriero, D. M. (2002) *Ann. Neurol.* **52**, 802–813.
8. Jin, K., Sun, Y., Xie, L., Peel, A., Mao, X. O., Batteur, S. & Greenberg, D. A. (2003) *Mol. Cell. Neurosci.* **24**, 171–189.
9. Zhang, R., Zhang, Z., Wang, L., Wang, Y., Gousev, A., Zhang, L., Ho, K. L., Morshead, C. & Chopp, M. (2004) *J. Cereb. Blood Flow Metab.* **24**, 441–448.
10. Palmer, T. D., Willhoite, A. R. & Gage, F. H. (2000) *J. Comp. Neurol.* **425**, 479–494.
11. Shen, Q., Goderie, S. K., Jin, L., Karanth, N., Sun, Y., Abramova, N., Vincent, P., Pumiglia, K. & Temple, S. (2004) *Science* **304**, 1338–1340.
12. Jin, K., Zhu, Y., Sun, Y., Mao, X. O., Xie, L. & Greenberg, D. A. (2002) *Proc. Natl. Acad. Sci. USA* **99**, 11946–11950.
13. Kovacs, Z., Ikezaki, K., Samoto, K., Inamura, T. & Fukui, M. (1996) *Stroke* **27**, 1865–1873.
14. Curtis, M. A., Penney, E. B., Pearson, A. G., van Roon-Mom, W. M., Butterworth, N. J., Dragunow, M., Connor, B. & Faull, R. L. (2003) *Proc. Natl. Acad. Sci. USA* **100**, 9023–9027.
15. Jin, K., Peel, A. L., Mao, X. O., Xie, L., Cottrell, B. A., Henshall, D. C. & Greenberg, D. A. (2004) *Proc. Natl. Acad. Sci. USA* **101**, 343–347.
16. Gould, E., Reeves, A. J., Graziano, M. S. & Gross, C. G. (1999) *Science* **286**, 548–552.
17. Kornack, D. R. & Rakic, P. (2001) *Science* **294**, 2127–2130.
18. Chen, J., Zhang, Z. G., Li, Y., Wang, Y., Wang, L., Jiang, H., Zhang, C., Lu, M., Katakowski, M., Feldkamp, C. S. & Chopp, M. (2003) *Ann. Neurol.* **53**, 743–751.
19. Zhang, R., Wang, Y., Zhang, L., Zhang, Z., Tsang, W., Lu, M. & Chopp, M. (2002) *Stroke* **33**, 2675–2680.